Noname manuscript No.
(will be inserted by the editor)

Alexander K. Hartmann

Ground states of two-dimensional Ising spin glasses: fast algorithms, recent developments and a ferromagnet-spin glass mixture

June 23, 2011

Abstract Using advanced numerical approaches based on optimization algorithms, much progress has been achieved for the study of the ground-state and low-temperature behavior of two-dimensional Ising spin glasses. Recent results led to a rather good understanding of these systems in the framework of the droplet-scaling theory. In this work, a pedagogical description of such an optimization-based approach is given and a short review of corresponding recent results is presented.

Furthermore, original results are presented for a special type of system which combines a ferromagnetic sub lattice with a spin-glass sub lattice. Results for exact ground-state calculations up to system size $N = 1448 \times 1448$ are given. Past results of similar systems gave evidence that such a system might exhibit a spin-glass phase at finite temperatures. Nevertheless, the present results do not support this notion. But, for a suitable balance between ferromagnetic and $\pm J$ spin-glass couplings, extremely large finite-size effects occur, which make the system look as if it orders if one studied just intermediate system sizes. Furthermore, although the system exhibits only a discrete set of interactions, a power-law behavior for the stiffness energy can be observed clearly for a large range of system sizes, in contrast to past systems with discrete sets of bond values.

key word: spin glasses; ground states; optimization algorithms; matching algorithms; domain walls; droplets; SLE processes

1 Introduction

During the last four decades, spin glasses (SGs) [15,65,35] have been one of the major research areas in condensed matter and statistical physics. Al-

Institut für Physik, Universität Oldenburg,
26111 Oldenburg, Germany
E-mail: a.hartmann@uni-oldenburg.de

though much progress has been achieved, there exist still many unsolved questions regarding the low-temperature behavior of SGs, in particular in finite dimensions [69]. Analytically, only few models can be treated, hence much effort has been put into numerical approaches [45], in particular Monte Carlo simulations [70,57]. Nevertheless, due to the issue of equilibration, only systems with a moderate number of spins can be treated. During the last decade, several mappings of the spin-glass ground state (GS) problem to combinatorial optimization problems [50] have been developed, which has allowed to study much larger systems. Here, it is explained for the particular case of two-dimensional Ising spin glasses, how GS and low-energy excited configurations can be obtained using so-called *matching algorithms* from graph theory. This allows to treat much larger samples compared to Monte Carlo simulations, even if Monte Carlo methods are combined with advanced techniques [83].

The SG model considered here [31,86] consist of N Ising spins $\sigma_i = \pm 1$ placed on a regular lattice or, in general, on the sites of a graph. The Hamilton function is given by

$$H \equiv -\sum_{\langle i,j \rangle} J_{ij}\sigma_i\sigma_j. \tag{1}$$

The sum $\langle i,j \rangle$ runs over all pairs of interacting spins, i.e., the edges of the graph, and J_{ij} denotes the strength of the bond connecting spins i and j. For each realization of the disorder, the values J_{ij} of the bonds are drawn according to a given probability distribution. Very common are the Gaussian distribution and the bimodal $\pm J$ distribution, which have the following probability densities, respectively:

$$p_{\mathrm{G}}(J) = \frac{1}{\sqrt{2\pi}} \exp\left(-\frac{J^2}{2}\right) \tag{2}$$

$$p_{\mathrm{bm}}(J) = 0.5\delta(J-1) + 0.5\delta(J+1) \tag{3}$$

Once the values of the bonds are fixed for a realization, they keep their values throughout the whole calculation or simulation, this is called *quenched disorder*.

If the underlying interaction graph is regular, one speaks of the Edwards-Anderson (EA) model [31]. On the other hand, the mean-field (MF) version of the model, involving interactions between all pairs of spins, was introduced by Sherrington and Kirkpatrick (SK) [86]. For a Gaussian distribution of the interactions, the SK model has been solved analytically through the use of several enhanced techniques by Parisi in the 1980s [65]. The main property of the solution is that a complicated energy landscape is obtained which organizes in the thermodynamic limit the state-space hierarchically using infinitely many levels. In particular, there are many low-energy states which are mutually very different from each other.

One of the great unsolved questions in spin-glass physics is, whether, or to what extent, the properties of the MF model are present also for finite-dimensional SGs. There is an opposing theory, the so called *droplet* picture

[60,22,36,37,19]. The droplet picture assumes that the low-temperature behavior is governed by droplet-like excitations. A droplet consists of a compact area of spins which are reversed with respect to a GS. Typical excitations of linear spatial extent l are assumed to cost an energy

$$\Delta E \sim l^{\theta} \ , \tag{4}$$

θ being a characteristic exponent. Note that *typical* here means that they dominate the thermodynamic behavior. This means, at finite temperature, that a droplet has minimum free energy for a given length scale l of the droplet. For $T = 0$, the minimum free energy requirement translates to a minimum-energy condition. The surface of a droplet is assumed to have a fractal dimension $d^s < d$, where d is the space dimension. Note that the surface of the droplet is at the same time a domain wall (DW) in the system, separating the spins having one ground-state orientation from the domain of spins having the opposite orientation. Furthermore it is usually assumed that the scaling behavior of the energy ΔE of different types of excitations, e.g. droplets and other domain walls, which can e.g. be induced by changing the boundary conditions, are described by the same exponent θ. The similarity and simplicity of all excitations means that the energy landscape is dominated by two large valleys, with the two GSs at the bottoms of these valleys.

In this work, results are reviewed for the two-dimensional ($d = 2$) model, obtained during the last decade using exact GS matching algorithms. These results strongly support the droplet picture for two-dimensional SGs. Note that results from finite-temperature simulations are not covered here. Throughout this work, systems with periodic boundary conditions in one direction will be considered. The paper is organized as follows: In section 2, some algorithms used to obtained exact GSs as well as domain-wall and droplet excitations are explained in a pedagogical stile. In section 3, the main results from these calculations will be exposed. In the fourth section, new results for a system with a mixture of a regular ferromagnetic sub system with a spin-glass sub system are shown. In the last section, a summary is given.

2 Algorithms

In general, the calculation of a spin-glass GS is an NP-complete problem [7]. Thus, so for only worst-case exponential-time algorithms are known. For GSs, the fastest known approach is the Branch-and-Cut algorithm [87,88].

Nevertheless, to calculate exact ground states and corresponding excitations of two-dimensional Ising SGs, polynomial-time algorithms [14,30,8,75, 67,50,91,76,64] are available, which allows to treat large system sizes. Here, a standard approach is explained, which is based on a direct mapping to a *matching problem*. This approach works for planar spin glasses and was used to obtain many of the recent results supporting the droplet picture. To explain the algorithms, some notions from graph theory [89] are needed, which will be given first. Next, the algorithm to obtain ground states is presented. Finally, the extensions of the algorithm needed to calculate excitations are exhibited. The presentation in this section is a concise but still pedagogical version of the extensive presentation of Ref. [43].

2.1 Graphs

A finite undirected *graph* $G = (V, E)$ is a finite set V of *vertices* (or *nodes*) connected by a set $E \subset V^{(2)}$ of undirected *edges* (or *links*). Hence, each edge $\{i, j\}$ is a set of exactly two vertices.

A *path* from v_1 to v_k is a sequence (ordered set) of vertices $v_1, v_2, \ldots, v_k$ which are connected by edges in the graph: $\{v_i, v_{i+1}\} \in E \ \forall i = 1, 2, \ldots, k-1$. If no node except the first and the last one appears twice in a closed path ($v_1 = v_k$) it is called a *cycle*. A *matching* is a subset $M \subset E$ of edges such that each vertex is contained in at most one edge. For a *perfect matching*, each vertex is contained in exactly one edge of M.

A weighted graph $G = (V, E, \omega)$ is a graph with edge weights $\omega : E \to \mathbb{R}$. The weight of a subset of edges, like a path S or matching M, is the sum of the weights of the edges contained in the subset. Hence, a *minimum-weight* path (also called *shortest path*) connecting v_1, v_k is the path connecting v_1 and v_k which has minimum weight. In the same way, a *minimum-weight* (perfect) matching is a (perfect) matching of minimum weight

2.2 Ground states

Now, we turn back to the planar two-dimensional spin glasses and show step-by-step how the calculation of GSs of (1) can be mapped on the minimum-weight perfect matching problem [14]. Note that the following explanation is given by considering a square lattice, but in fact the algorithms can be applied to general planar lattices. Thus, also systems with honeycomb or triangular lattices can be treated in the same way. We start with the two-dimensional SG with free boundary conditions in all directions, shown in Fig. 1.

We assume a configuration where all spins are "up", i.e., $\sigma_i = +1 \ \forall i \in V$. This means all ferromagnetic bonds will be satisfied, since all pairs of interacting spins exhibit in the same orientation, while all antiferromagnetic bonds are not satisfied. Since there are 25 ferromagnetic bonds with $J_{ij} = +J$ and 15 antiferromagnetic bonds with $J_{ij} = -J$, the total energy of the configuration is $E = -25J + 15J = -10J$. Now we draw dashed lines perpendicular to all non-satisfied bonds, the result is shown in Fig. 1.

This set of perpendicular dashed lines can be seen as a subset of edges in a new *dual* graph $G' = (V', E')$, which is now defined. The vertices of G' consist of the set of all elementary cycles p with four edges, i.e., of length four. These cycles are called *plaquettes*. As we will see below, of particular importance are *frustrated* plaquettes, which are defined as those plaquettes which contain an odd number of negative bonds. In general a set of plaquettes is defined as a (non-unique) subset P of all cycles of a graph such that each possible cycle can be composed from a symmetric difference (i.e. $A \Delta B = (A \cup B) \setminus (A \cap B)$ for sets A, B) of members from P. One can show [14], that a set $L \subset E$ of unsatisfied bonds is physical, i.e., corresponds to a spin configuration, if each frustrated (unfrustrated) plaquette contains an odd (even) number of edges in L. In case of free boundary conditions in all directions, as in the graph in Fig. 1, also the "large" cycle surrounding the system, i.e. consisting of

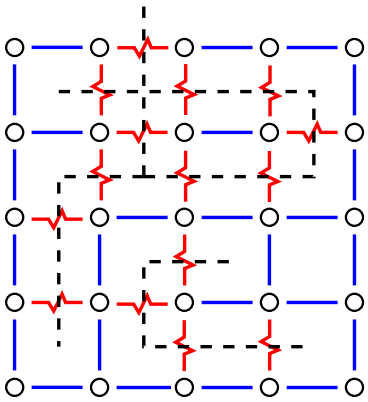

Fig. 1 The two-dimensional spin glass, having free boundary conditions in all directions. Empty circles represent spins. The solid lines represent ferromagnetic bonds, the jagged lines antiferromagnetic bonds. All spins are assumed to be "up" $\sigma_i = 1$. Dashed lines are drawn perpendicular to unsatisfied edges, which are the antiferromagnetic edges in this case.

the boundary spins of the full system, is a member of V', while for periodic boundary conditions only in the x direction, also the two cycles containing all spins at the top and all spins at the bottom, respectively, are added. By adding these one or two "extra" plaquettes, each bond of the original graph is contained in exactly two cycles of V'. This allows to choose the edges in E' as those elements $\{p_1, p_2\}$ where in the original graph G, the plaquettes p_1 and p_2 have exactly one bond in common (denoted as $J(p_1, p_2)$) i.e. all neighboring plaquettes. Since each edge $\{p_1, p_2\}$ in G' corresponds exactly to the bond $J(p_1, p_2)$ crossed in G, we can assign also weights to the edges of G' by choosing $w'(\{p_1, p_2\}) = |J(p_1, p_2)|$. It will be shown below that this choice is useful. As an example, in the left of Fig. 2, the resulting graph G' for G from Fig. 1 is shown (without edge weights). Note that for the $\pm J$ model, we have the weight $w'(\{p_1, p_2\}) = J$ for all edges. In the right of Fig. 2 a dual graph G' for a graph similar to the graph Fig. 1 is shown, except that it has periodic boundary conditions in the x direction.

In Fig. 3, the graph from Fig. 1 is repeated, but now the vertices of G' are also shown. In addition, the frustrated plaquettes are marked by capital letters. Note that also the large plaquette A surrounding the system is frustrated. Hence, the set of dashed lines represents a subset $\mathcal{L}$ of edges from E'. Since they cross the bonds of G which are unsatisfied in configuration $\{\sigma_i\}$, we can rewrite the energy $H(\{\sigma_i\})$ as

$$\begin{aligned} H(\{\sigma_i\}) &= \sum_{e' \in \mathcal{L}} w'(e') - \sum_{e' \in E' \setminus \mathcal{L}} w'(e') \\ &= 2 \sum_{e' \in \mathcal{L}} w'(e') - \sum_{e' \in E'} w'(e') \\ &= 2w'(\mathcal{L}) - w'(E') \end{aligned} \tag{5}$$

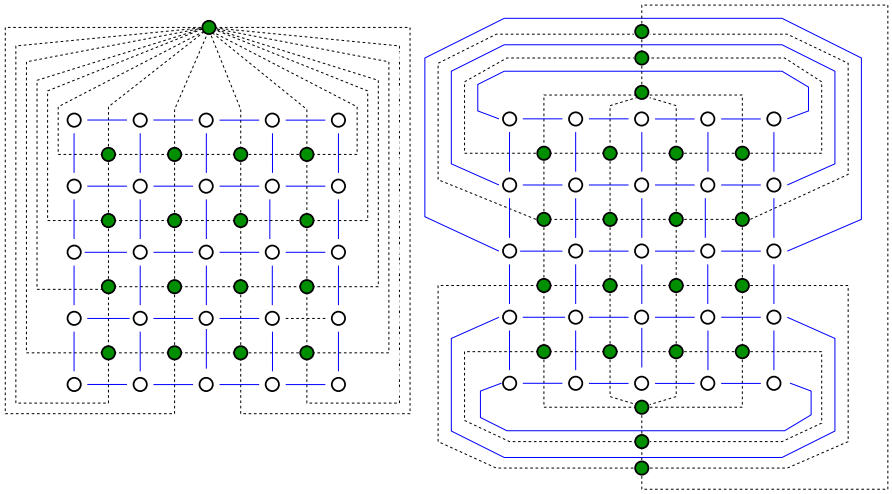

Fig. 2 Dual graphs G' for the spin glass. The plaquettes p are represented by filled circles inside the elementary cycles. The edges of the dual G' are denoted by dashed lines. Note that we draw the bonds of G here just as thin lines, irrespectively of their sign and magnitude. Left: for the graph from Fig. 1 (free boundary conditions in all directions). The large plaquette surrounding the system is represented by a circle outside the graph G. Right: for the case G had periodic boundary conditions in the x direction: two extra plaquettes are added, represented by the third filled circles from the top and from the bottom, respectively.

Therefore, in this expression each unsatisfied bond $\{i, j\}$ of the original graph G, corresponding to an edge $e' \in \mathcal{L}$, contributes a positive energy $w'(e') = |J_{ij}|$ and each satisfied bond, corresponding to an edge $e' \in E' \setminus \mathcal{L}$ contributes a negative energy $-w'(e') = -|J_{ij}|$. Note that in the second line, the second term is a constant which does not depend on the spin configuration.

If we now take a closer look at Fig. 3, we observe that *all* edges from $\mathcal{L}$ either are contained in paths joining frustrated plaquettes or they are contained in cycles. Here, we have paths from A to B, from C to E and from D to F, and a cycle of length 6 (shaded area). Note that this way to describe $\mathcal{L}$ via cycles and paths is not unique. Nevertheless, it is only important that different descriptions exhibit the same set $\mathcal{L}$, hence the same energy.

This description via cycles an paths joining frustrated plaquettes is not only valid for this special configuration $\sigma_i = 1$, but it is valid for *all possible* spin configurations. If we for example flip the second spin in the top row, we change the state of all neighboring bonds satisfied $\leftrightarrow$ unsatisfied. This means that the path connecting the frustrated plaquette B in the upper left corner with the frustrated plaquette A is just redirected, see upper right of Fig. 3. Previously, the weight of the path from A to B contributed two edges to $\mathcal{L}$ and a value $2J$ to $w(\mathcal{L})$, now it contributes just one edge and the weight J. Therefore, the total energy is decreased to $E = -26 + 14 = -12$. In a similar way the configuration changes, when in the third and fourth row the second

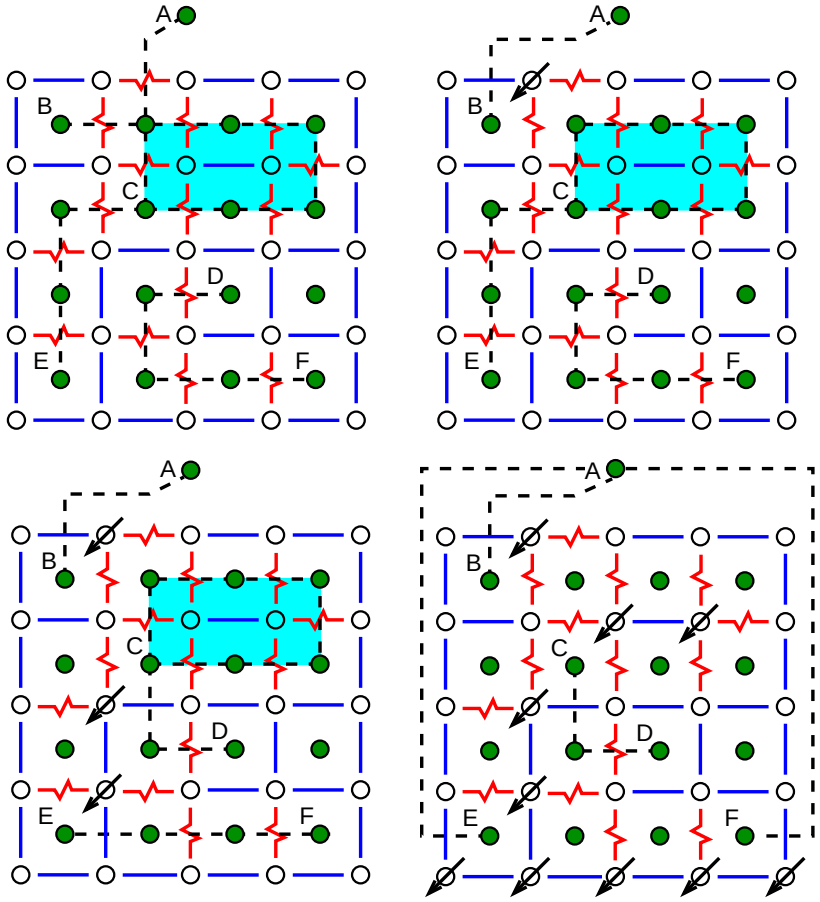

Fig. 3 The two-dimensional spin glass with free boundary conditions from Fig. 1. In the top left, all spins are assumed to be "up" $\sigma_i = 1$. Dashed lines indicate the edges present in the set $\mathcal{L}$ of the dual graph $G' = (V', E')$ (see text). All edges in E' are either contained in paths connecting frustrated plaquettes (denoted by capital letters) or in cycles (shaded area). In the top right, the situation is shown, which arises, when the second spin in the top row is flipped. In the lower left, in addition the second spins of the third and fourth row are flipped. In the lower right, a GS is shown.

spin is flipped, respectively, see lower left of Fig. 3. The resulting energy is $E = -28 + 12 = -16$

We are finally interested in obtaining a GS. Looking at (5), one observes that minimizing the energy is equivalent to minimizing the total weight $w(\mathcal{L})$ of edges in $\mathcal{L}$. We have already decreased the total weight by the spin flips shown before. Also, we can decrease the total energy always by removing *all* cycles in $\mathcal{L}$. This is achieved by just flipping all spins surrounded by each cycle. Here, when we flip the two spins in the shaded area, we remove 6 edges from $\mathcal{L}$, hence decreasing the energy to $E = -34 + 6 = -28$. It

becomes obvious that in a GS no cycle will exist. Hence, a ground-state configuration can be described by a set $\mathcal{L}$ of edges from E' which form paths connecting frustrated plaquettes. Each frustrated plaquette is connected to exactly one other frustrated plaquette. Finally, to minimize (5), these paths will be of minimum weight. If one calls the weights "distances", this means that the frustrated plaquettes are connected by shortest paths in the GS. We see that in the lower left Fig. 3, E and F are connected by a path of weight (distance) $3J$. This can be further decreased by flipping all spins on the bottom row, leading to a path of weight $2J$ from E to F. Note that the path now includes plaquette A. We observe that one has again alternative but equivalent descriptions of the situation, e.g. one could say that A to E and B to F are connected by paths in G'. The ground-state energy is $E = -35 + 5 = -30$.

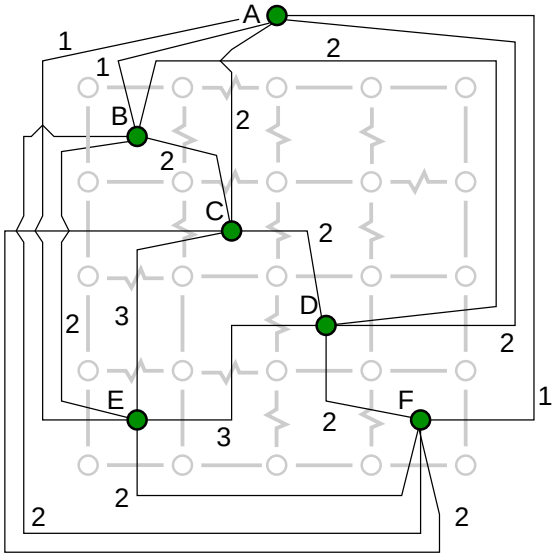

Fig. 4 The complete graph G'' of frustrated plaquettes obtained from G'. Each edge $\{f_1, f_2\}$ carries a weight w'' which is the minimum weight (shown in units of J) among all paths from f_1 to f_2 in G'. The edges are drawn in a way, that they cross the edges of G corresponding to a minimum weight. When interpreting the weights as distances, this is the length of a shortest path from f_1 to f_2. Note that for G', where all edge weights have value J, the length weight is just the number of edges.

To conclude, to obtain a GS, we just have to consider the frustrated plaquettes, and we have to look for paths connecting the frustrated plaquettes pairwise. Each frustrated plaquette is connected to exactly another frustrated plaquette. This means, we are looking for a perfect matching of frustrated plaquettes. Since the energy directly corresponds to the weight of the matching, we are looking for a minimum-weight perfect matching to obtain a GS. To formalize this, the graph $G'' = (F', F' \times F')$ is defined. The set F' of

vertices just contains the frustrated plaquettes from V', hence $F' \subset V'$. The graph G'' is a *complete* graph, because in $F' \times F'$ all possible edges $\{f_1, f_2\}$ ($f_1, f_2 \in F'$) are contained. We assign weights by choosing $w''(\{f_1, f_2\})$ as the weight of the minimum-weight (shortest) path from f_1 to f_2 in G'. Hence, to obtain the GS of the two-dimensional spin glass, *two* optimizations have to be performed.

- First, the calculation of all minimum-weight (shortest) paths in G' between all pairs of frustrated plaquettes. For this purpose a standard polynomial-time shortest-path algorithm, e.g. the Dijkstra algorithm can be used from the literature [85,29]. As example, in Fig. 4 the graph G'' obtained from G' for our example is shown.
- Second, a selection of the minimum-weight perfect matching of frustrated plaquettes, where the edge weights of the complete graph G'' are the minimum-weights of the paths obtained in the first step. The calculation of minimum-weight perfect matchings is a problem which can be solved quickly on a computer, meaning that the running time increases also only polynomially with the system size in the worst case. Again standard algorithms from computer science can be applied here [28,56]. Since these algorithms are rather complicated, at least in case of efficient implementations, we recommend to use existing computer programs from scientific libraries, e.g. the LEDA library [61] or the `blossom4` implementation within the Concorde library [27]. These algorithms have a running time $O(nm \log n)$ for a graph with n vertices (here $n = |F'|$) and m edges (here $m = |F' \times F'| = |F'|^2$).

Finally, a ground-state configuration can be obtained from the minimum-weight perfect matching. Exactly those bonds are not satisfied (in G), which are crossed by the minimum-weight paths in G' connecting the matched frustrated plaquettes (in G''). Note that due to the connection to shortest paths, due to the fact that each frustrated plaquette cannot be matched to more than one other plaquette and due to the minimality of the matching, it is impossible that more than one of the selected paths crosses a bond. The spins are then obtained, by first selecting (say) the upper-left spin either up or down. This corresponds to the trivial degeneracy due to the spin-flip symmetry of the Hamiltonian. Then one runs systematically through the lattice and sets neighbors of already set spins either to the same (if the connecting bond is satisfied ferromagnetic or unsatisfied antiferromagnetic) or the opposite (if the connecting bond is unsatisfied ferromagnetic or satisfied antiferromagnetic) orientation. Note that the minimum-weight paths are sometimes not unique. For example the path connecting plaquettes E to F can go through the bonds to the left or below of E, also either to the right or below of F. Hence, the ground-state spin configuration can also be non-trivially degenerate. Another source of degeneracy is that multiple minimum-weight matchings might exist, but not all different matchings lead to different spin configurations, see e.g. the lower right part of Fig. 3. More on how to treat degeneracy, you can find in Ref. [58]. Here, we are interested mainly in energetic aspects, where the spin configurations are not important.

Finally, a technical note is given. For a system of site $N = L \times L$, there are $O(N) = O(L^2)$ frustrated plaquettes. Since the graph G'' is complete,

it exhibits $m \in O(L^4)$ edges. This leads to a rather strongly increasing running time of $O(L^6 \log L^4)$, although it is still bounded by a polynomial. For the minimum-weight perfect matchings, one observes that for random samples, there are "almost never" edges in G'' with "large" weight contained in matchings. For thousands of samples of the $\pm J$ model, never a sample with a weight larger than $6J$ was observed in our studies. Hence, one can safely remove all edges from G'' with a weight larger than some $w_{\max}$ even while calculating the shortest paths. From numerical experiments, testing whether the result depends on $w_{\max}$, one finds that $w_{\max} = 6J$ is a safe value for the $\pm J$ and $w_{\max} = 8J$ for the Gaussian SG.[1]

2.3 Domain walls and droplets

As already indicated in the introduction, not only obtaining true ground states is interesting, but the calculation of excited states using GS algorithms is one major task to understand the behavior of two-dimensional spin glasses. One possible general approach consists of these three steps:

1. Calculate the GS $\{\sigma_i^{(0)}\}$ of a given realization and the GS energy E_0.
2. Modify some of the couplings.
3. Calculate the GS $\{\sigma_i^{(m)}\}$ of the modified system, which is usually a low-lying excited state of the original realization. The ground-state energy of the modified sytsem is denoted by $E_0^{(m)}$. The energy with the original bonds of the configuration $\{\sigma_i^{(m)}\}$ is denoted by $E_1^{(m)}$.

Note that the algorithm presented in the last chapter breaks the spin-flip symmetry by choosing the upper left spin "up", hence indeed a unique GS can be assumed here. Here, we will consider two types of excited states, *domain walls* and *droplets*, which play a major role in the theoretical study of SGs. Other types of excitations, which can be generated using ground-state algorithms in the same spirit, are discussed in the literature [67,74,52,49].

A DW spanning the whole system can be generated, e.g. by switching the boundary conditions from periodic to antiperiodic in one direction. This is done by taking one column of bonds, e. g., those which "wrap around the system boundaries", and by then inverting the signs of all bonds in this column, see Fig. 5.

After calculating the GS with the modified system, the pairs of spins touching most[2] of the modified bonds will have a relative orientation to each other, which is different from the GS obtained with the original bonds previously. In this way two domains are generated; one, where the spins have their GS orientation; another, where the spins have opposite sign with respect to the GS. Note that *inside* the domains, all pairs of adjacent spins

[1] that there are more general models, e.g. the $\pm J$ random bond model, where the fraction of ferromagnetic and antiferromagnetic bonds is not equal. For those models, usually $w_{\max}$ must be a bit higher.

[2] The DW generated might cross the modified bonds. At these few positions, the adjacent spins have still the relative GS orientation.

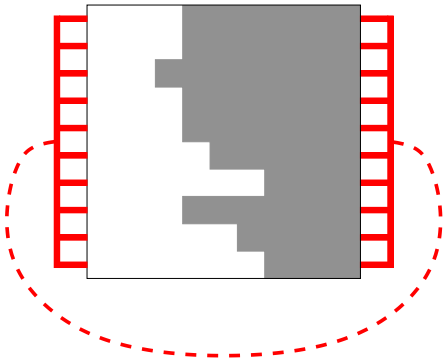

Fig. 5 Method used to generate DWs. After calculating the GS, the signs of all bonds connecting the pairs of spins in the first and last column (represented here by the thick broken line) are inverted. In this way two domains are generated; one, where the spins still have their GS orientations (indicated by the light area); another, where the spins have opposite sign with respect to the GS (dark area). Note that the DW separating the two domains runs not necessarily "in the middle" of the system. Hence for some realizations, the DW might even cross the line of inverted bonds.

still have the relative GS orientation to each other. The two domains are separated by the DW [3], which will adjust in a manner that the total energy is minimized. Hence, the GS energy of the modified system is locally everywhere the same as in $\{\sigma_i^{(0)}\}$, except at the DW. Thus, when calculating the energy difference between the GS energies E_0 of the original GS configuration and $E_0^{(m)}$ of the modified configuration, one obtains exactly the energy of the DW: $\Delta E \equiv E_0^{(m)} - E_0$.

Now we turn to the second kind of excitation discussed here, i. e., droplets. As mentioned in Sec. 1, droplets are connected clusters of spins, which are reversed with respect to the GS, and which are of minimum free energy. For $T = 0$, the minimum free energy requirement translates to a minimum-energy condition. This allows us to verify the scaling assumption (4) of the droplet scaling theory by GS calculations. We will consider two-dimensional spin glasses with free boundary conditions for the rest of this chapter.

A traditional approach of generating droplets was used by Kawashima and Aoki within a Monte Carlo simulation [54]. They first calculated the GS heuristically with an algorithm based on gradually "cooling" the system. Then they recalculated the GS with the constraints that the spins on the boundary keep their GS orientation, while a central spin is flipped, see Fig. 6. Fixing the spins can be achieved by introducing strong local fields acting on the spins, with the direction of the fields chosen to point along the desired direction, hence one has to apply a Hamiltonian with a linear field

[3] Formally, when comparing with the original GS, the two domains are also separated by a second DW which is just a straight line along the modified bonds, but this DW does not contribute to the energy change.

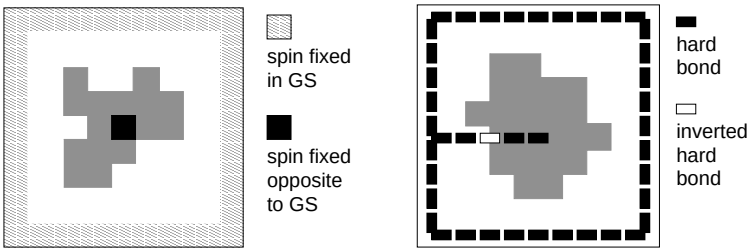

Fig. 6 Left: Basic method to generate a droplet. After calculating the GS, fix the spins at the boundary in their GS orientation and fix one central spin in opposite GS orientation. A GS calculation with the fixed spins results in a droplet (black/grey area), consisting of spins opposite to the original GS orientations (white/shaded area). Right: Method used to generate the *cross* droplets. After calculating the GS, several hard bonds (thick lines) are introduced, one hard bond is inverted (see triangle), leading to the appearance of an excitation (dark inner area).

term.[4] Since the droplet energy decreases with droplet size (since $\theta < 0$), for each given system the droplets become typically as large as possible at small temperature. Hence, this approach generates droplets of the order of the system size, i. e., $l \sim L$. Using this approach, small systems up to $L = 50$ with a Gaussian distribution of the interactions could be studied, and a scaling $\Delta E \sim L^{\theta'}$ of the droplet energy with $\theta' = -0.45(1)$ was found, which is significantly different from $\theta \approx -0.28$ obtained for domain walls, see next section.

Since the range of system sizes in the work of Kawashima and Aoki is limited to $L \leq 50$, their result might have been an artifact of too-small sizes. Using matching algorithms, one can study much larger sizes. Unfortunately, it is not possible to treat local magnetic fields, i. e., one cannot fix a spin in some orientation. But it is possible to mimic this kind of generation of droplets in the following way. After obtaining the GS, several *hard bonds* are introduced. A hard bond is a bond with a high value of the absolute strength (one can imagine $J_{\rm big} \sim 10^5 J$ or $J_{\rm big} = 2N \times \max_{\langle i,j\rangle}\{J_{ij}\}$). The strength of a hard bond is so large such that the bond will be satisfied in *all* subsequent GS calculations.[5] Most of the hard bonds are used to ensure that neighboring spins i_0, j_0 have the same relative orientation as in the GS $\{\sigma_i^{(0)}\}$, i. e., one replaces bond $J_{i_0 j_0}$ by a bond with the value $J'_{i_0 j_0} = J_{\rm big}\sigma_{i_0}^{(0)}\sigma_{j_0}^{(0)}$. An *inverted* hard bond has the opposite sign, i. e., it forces two neighboring spins to take orientations, which are different relative to their GS orientations. This means in a GS calculation with the inverted hard bond, one of the two spins will flip with respect to $\{\sigma_i^{(0)}\}$, the other spin will keep its previous GS orientation. Note that the subsystem of all hard bonds together must not

[4] Alternatively, one can just ignore the fixed spins in the second GS calculation and leave their current orientations. Then the fixed spins act as local fields to their neighbors.

[5] When working with a maximum weight $w_{\rm max}$ of the edges in the graph G'' of frustrated plaquettes, see end of last section, it is sufficient to chose $J_{\rm big} > w_{\rm max}$.

exhibit frustration, because no hard bond should be broken when a new GS is calculated.

Now we describe in detail which hard bonds are introduced to obtain droplets. First, all boundary spins are fixed relative to each other by introducing hard bonds around the border, see Fig. 6. The signs of these hard bonds are chosen such that they are compatible with the GS orientations of the spins they connect. This keeps the spins on the boundary in their GS orientations. Another line of hard bonds is created which runs from the middle of (say) the left border to a pre-chosen center spin, again fixing the bond's spins in their relative GS orientations. Next, the sign of exactly *one* hard bond on this line is inverted. Now a GS of the modified realization is calculated. With respect to the original GS, the result is a minimum energy excitation, fulfilling the constraints that it contains the center spin, does not run beyond the boundary and that it has a surface which runs through the hard bond which has been inverted. Hence, it will be a constrained droplet.

Note that this procedure alone does not generate the droplets as defined above, because the border of the droplet is constrained to run through the inverted hard bond, while it can fluctuate freely for the original droplets. Therefore, for each realization, this procedure is iterated over all the bonds which are located on the line from the boundary to the center, when in each case exactly one hard bond is inverted. Among all $L/2$ excitations generated in this way, the one exhibiting the lowest energy $E_1^{(m)} - E_0$ (i.e., both $E_1^{(m)}$ and E_0 calculated with the original bonds) is selected as the minimum energy droplet. Hence, the DW of a such defined droplet must cross the imaginary line between the left boundary and the center spins exactly once, and may fluctuate freely everywhere else. Therefore, to introduce even more flexibility of the DW, the full procedure is iterated over all four choices of lines of bonds running from the left, right, top and bottom boundary to the center spin. This means, for each realization finally the true minimum droplet is selected as that one having the minimum energy among all $2L-2$ excitations generated in this way. This approach generates droplets, called *cross droplets*, which are very similar to the droplets of Kawashima and Aoki, except that no droplets can be generated, where the boundary fluctuates freely in all four directions at the same time. However, it was found that these strongly fluctuating droplets play a minor role [48], their influence on the final result is smaller than the fluctuations resulting from the statistics.

Note that one can study also other types of excitations [52], which are obtained, e.g., by just slightly changing the bonds after the first GS calculation. Furthermore, one can use the concept of hard bonds and GS calculation, by iterating the algorithms in a hierarchical way, to obtain a low-energy path from a ground state to its inverted counterpart [3]. For details, please consult the cited references.

3 Review of main recent results

In the following, results of GS calculations concerning scaling behavior of energy, domain walls, and droplets are reviewed. Also results for other types

of excitations, energy barriers and test concerning Schramm-Loewner evolution (SLE) behavior [25] are mentioned. Throughout this work, systems with periodic boundary conditions in one direction will be considered, except for the droplet calculations, where the boundary conditions are free.

First, one is interested in domain walls, because their creation roughly corresponds to a real-space renormalization [39,24] of the system [20]. By averaging over this renormalization one obtains a renormalized distribution of coupling strengths. A measure for the strength of the interaction distribution will be the width of the distribution $\Delta = \sqrt{\mathrm{Var}(\Delta E)}$, called *stiffness* here. From simple scaling arguments by Bray/Moore and McMillan [20,60] and in numerical experiments one finds a power-law behavior $\Delta \sim L^{\theta}$, where θ is the droplet exponent, also called *stiffness exponent* in this context. Hence, the scaling is the same as for the droplet scaling Eq. (4), but with the droplet size replaced by the system size. If $\theta < 0$, then the interactions become weaker with increasing size of the renormalized region. This means, in the limit of an infinitely large region, the spins are effectively no longer coupled, hence the system behaves paramagnetically at any finite temperature, i.e. $T_c = 0$. This is indeed the case, as we will see next. Note that there is also analytical evidence obtained by Ohzeki and Nishimori [71], that $T_c = 0$ for $d = 2$ SGs.

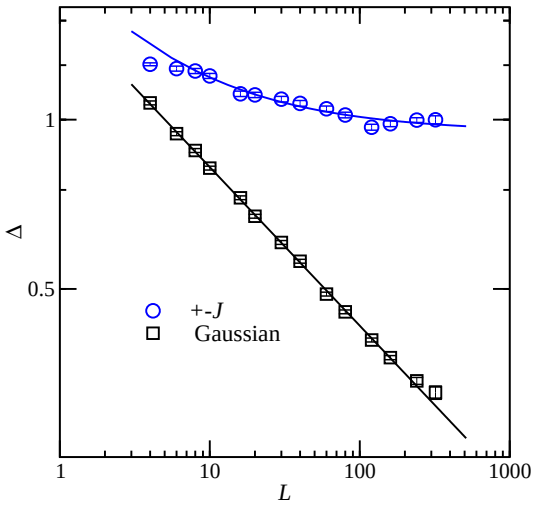

Fig. 7 Width of the stiffness-energy distribution for the standard spin glass with Gaussian and bimodal distribution of the bonds, respectively. The solid lines show fits to functions $\Delta(L) \sim \Delta_\infty + bL^{\theta}$ with $\Delta_\infty = 0.95(2)$, $b = 0.93(24)$, $\theta = -0.59(15)$ ($\pm J$) and $\Delta_\infty \equiv 0$, $b = 1.58(1)$, $\theta = -0.282(2)$ (Gaussian). See also Ref. [51].

A couple of results to obtain the stiffness exponent were published, using exact transfer-matrix approaches by Bray/Moore and McMillan [20,59] or Branch-and-Cut algorithms by Rieger et al. [80], but restricted to small system sizes. By using the matching approach much larger systems can be treated. In Fig. 7 the resulting stiffness Δ is shown as a function of system

size L for the Gaussian distribution Eq. (2) and the $\pm J$ distribution Eq. (3). The data is from Ref. [51]. For the Gaussian case, a clear power law with exponent $\theta_{\rm G} = -0.282(2)$ is visible, while for the $\pm J$ case the stiffness saturates at a value around 1, leading to $\theta_{\rm bm} = 0$. These results indicating a non-universality between Gaussian and bimodal $\pm J$ distribution were supported later on by Amoruso et al. [4] via detailed calculations for Migdal-Kadanoff lattices. They showed that for this type of lattice the lower critical dimension is different for the two kinds of distributions. In Ref. [51] a slightly different value for $\theta_{\rm G}$ was obtained for a different type of boundary conditions, when the boundary conditions were switched from free/free (x/y) to antiperiodic/free. The aspect-ratio approach, as introduced for spin glasses by Carter, Bray and Moore [26], consists of performing calculations for systems of various aspect ratios L_x/L_y. Using this approach it was shown [46] that the apparent boundary-condition dependence is a finite-size artifact. As a result, the boundary-condition independent value of $\theta_{\rm G} = -0.287(4)$ was determined. When studying [17] exact GSs of diluted lattices, which allows in combination with a reduction method introduced by Boettcher [16] to go in principle to even larger system sizes, a value $\theta_{\rm G} = -0.281(1)$ was found.

Several authors addressed the fractal properties of domain walls. In early works [21,80,73], using exact transfer-matrix and Branch-and-Cut approaches, only small system sizes could be treated, resulting in estimates $d_{\rm G}^{\rm s} \approx 1.26(3)$ ... 1.34(10). Later on matching algorithms were used [62], resulting in a higher accuracy: For the Gaussian model, a fractal surface dimension of $d_{\rm G}^{\rm s} = 1.274(2)$ was obtained. This is compatible with other results [54,68, 12] which were also obtained by using matching algorithms but with somehow lower accuracy. Basically the same value $d_{\rm G}^{\rm s} = 1.273(3)$ was found also for large systems sizes independently by Weigel and Johnston [92]. Due to the degeneracy of the GS, determining the fractal properties is more difficult for the bimodal model. Here, using extensions of the algorithm which favor short and long domain wall, limits $1.095(2) \leq d_{\rm bm}^{\rm s} \leq 1.395(3)$ where found. An estimate $d_{\rm bm}^{\rm s} = 1.30(1)$ for the bimodal model was obtained for sizes $L \leq 100$ by Romá et al. [82] by using a matching approach, which unfortunately suffers from non-uniform sampling. Later Risau-Gusman and Romá [81] refined this value for small systems by using either Monte Carlo ($d_{\rm bm}^{\rm s} = 1.33(1)$), which seems to sample uniformly, or again by a non-uniform-sampling matching approach for sizes $L \leq 300$ ($d_{\rm bm}^{\rm s} = 1.323(3)$). Hence, the authors concluded that the value of the fractal dimension seems to not be significantly affected from non-unifrom sampling. Anyway, recently a new approach was proposed by Thomas and Middleton [91], which enables the true sampling of degenerate ground states. So far it has been used to determine GS energies. Nevertheless, this algorithm could be used in the future to determine accurately the fractal surface dimension for the bimodal model. Furthermore, the degeneracy of the bimodal $d = 2$ SG has be explored partially [84] by calculating bonds, which have in all GSs the same state satisfied/unsatisfied, respectively. For this study an algorithm [9,79] to calculate the backbone of a system was applied, but in conjunction with Monte Carlo approach for the GS calculations. Therefore, this the study was limited to rather small system sizes. Nevertheless, the method [9] could easily be used within the matching approach. Note

that Atisattapong and Poulter [6] studied an Ising spin glass on a special lattice, the *brickwork lattice* with spin-coordination number three, where the degeneracy seems to be finite.

Note that similar and consistent results on the behavior of domain walls, but not to that extent, were obtained in several studies [72,55,1,34,63] for the two-dimensional Ising random-bond model. For this model, one studies systems with a variable fraction of negative bonds, such that one can tune the system between an (anti-) ferromagnetic and a ($T = 0$) spin-glass region. Note that for the random-bond model also triangular lattices [10,11,64] were studied. Hence, the $T = 0$ behavior of two-dimensional Ising SGs seems to be universal with respect to the actual concentration of frustrated plaquettes, as long as spin-glass behavior emerges.

Interestingly, θ shows up within even simpler calculations: The most simple thing one can do when calculating spin-glass ground states is to study the dependence of the average GS energy $e(L)$ per spin on the system size L. It was argued by Bouchaud, Krzakala and Martin [18] that the behavior should be governed by the droplet exponent θ. Indeed, in Ref. [23], for the Gaussian system Eq. (2), a behavior was found which is compatible with

$$e(L) = e_\infty \left(1 - L^{-(2-\theta_{\mathrm{G,e}})}\right) , \tag{6}$$

as predicted. The best-fit values are $e_\infty \approx -1.31479$ and $\theta_{\mathrm{G,e}} = 0.281(7)$, which is compatible with the numerical results for the domain-wall calculations. The reason that θ appears in this equation, although no excitation seem to be created, is the presence of periodic boundary conditions in (at least) one direction. The same system with fully free boundary conditions would have a lower energy and a different ground-state configuration. The periodic boundary conditins introduce additional boundary-induced frustration which leads to the (hidden) appearance of domain-walls, compared to the system with fully free boundary conditions. Hence, for a very simple set up, already the droplet-scaling exponent can be observed, as it will be obvious by comparing with the results presented below. For the $\pm J$ model Eq. (3), a behavior according Eq. (6) with $\theta_{\mathrm{bm,e}} \approx 0$ was found, also compatible with the domain-wall result for this system. Nevertheless, the data matched to the function less well, which indicates that stronger finite-size corrections were present. This is also certainly the case for droplets, which are discussed next.

The average droplet energy data obtained using the matching approach [49,48,44] is shown in Fig. 8. For the Gaussian case, for small system sizes, a rather step decrease following a power law $L^{\theta'_{\mathrm{G,d}}}$ with $\theta'_{\mathrm{G,d}} = -0.47$ is observed. This is compatible with previous results by Kawashima and Aoki and with the results of Picco, Ritort and Sales [77], both for droplet-type excitations of limited system sizes. Consequently, these authors claimed that domain walls and droplets behave differently. Nevertheless, when going to larger sizes one can observe a crossover to a behavior $L^{\theta_{\mathrm{G,d}}}$ with $\theta_{\mathrm{G,d}} = -0.29$, compatible with the above state value $\theta_{\mathrm{G}} = -0.287(4)$. Hence, one needs large system sizes to observe the true limiting behavior. Nevertheless, for droplets with volume constraints, compatible results were obtained by Berthier and Young [13] for even smaller system sizes $L \leq 64$.

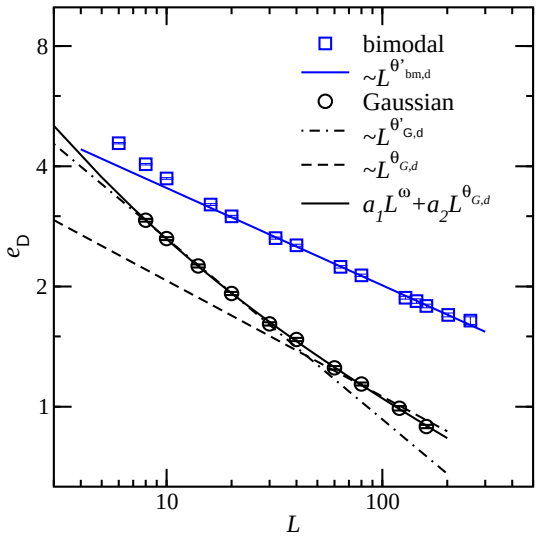

Fig. 8 Average droplet energy for bimodal $\pm J$ (squares) and Gaussian (circles) systems. The lines show different types of functions, see figure, with $\theta'_{\rm bm,d} = -0.25$, $\theta'_{\rm G,d} = -0.47$, $\theta_{\rm G,d} = -0.29$, $\omega = -1$, $a_1 = 6.86$, $a_2 = 3.69$.

Interestingly, although the stiffness exponent $\theta_{\rm bm} = 0$ for the bimodal $\pm J$ case is different than from the value for the Gaussian system, droplets seem the be governed by the same power law: As Fig. 8 shows, the raw data for the bimodal model exhibits a $L^{\theta'_{\rm bm,d}}$ ($\theta'_{\rm bm,d} = -0.25$) behavior. Kawashima showed [53] than one has to take into account that these droplets have a volume fractal structure with a fractal exponent [44] $D_V \approx 1.81 < 2 = d$. This value is only an estimate, since the algorithms used so far are not able to handle the exponential degeneracy of the GS for the bimodal model correctly (i.e., via sampling uniformly). Note that for the Gaussian system the droplets are compact ($D_V = 2$). Using Kawashima's correction for the fractal structure one obtains a value which is also compatible with the Gaussian value: $\theta_{\rm bm,d} = \theta'_{\rm bm,d} d/D_V \approx -0.28$. The fact that for the bimodal case droplets and domain walls are characterized by different exponents $\theta_{\rm bm,d} \approx -0.29/\theta_{\rm bm} = 0$ can be understood by simple scaling arguments [44], where the probability that a zero-energy droplet exists is related to the probability of a zero-energy domain wall. The main point is that for a droplet to have non-zero energy, (closed) domain walls containing the center spin on all lengths scales must have non-zero energy.

Also the surface fractal properties of the droplets for the Gaussian model were determined [48] and a value of $d^s_{\rm G,d} = 1.1(1)$ was found. This is a bit lower than the result found for the domain walls, but not out of reach given the error bar. The reason for the difference is probably that for the droplets only smaller systems could be considered, due to the higher computational complexity. Hence, finite-size effects are likely to be stronger. For the bimodal

model, due to the degeneracy, no accurate surface fractal exponent of droplets could be determined so far.

The droplets discussed so far correspond basically to the assumptions made in the droplet theory. But, as mentioned at the end of section 2.3, other ways to create droplet excitations exist. For the Gaussian model Eq. (2) for three different types of these droplets the stiffness exponent θ and the fractal dimension d^s was determined [52]. For the stiffness exponent, values slightly lower than the value of $\theta_{\mathrm{G}} \approx -0.287$ were obtained (around -0.34), which was probably due to the limited range of system sizes considered in Ref. [52]. For the fractal surface dimension $d^s \approx 1.33$ was found, slightly above the values found for domain walls of much larger systems. Also it should be mentioned that a fundamentally different type of "excitation" can be studied when performing repeated GS calculations for window subsystems, as, e.g., done for triangular lattices [67].

To summarize, the so far reviewed results show that indeed the droplet theory seems to hold for two-dimensional Ising spin glasses: The energy landscape is rather simple. The low temperature behavior is dominated by droplet-type excitations above the ground state. Different types of excitations like domain walls and various kinds of droplets are, for the Gaussian distribution, universally described by the same stiffness exponent $\theta \approx -0.287$ and they have the same fractal surface dimensions. For the bimodal distribution (and likely other discrete distributions), large scale domain walls and droplets are described by different stiffness exponents, which can be understood by simple scaling arguments. Nevertheless, droplet excitations, which are responsible for the thermodynamic low-temperature behavior, exhibit the same properties for Gaussian and bimodal distribution.

By using matching algorithms, also much more complex studies were performed. For example, the scaling of the energy E_{barrier} of lowest energy barrier separating a ground state and its inverted counterpart was studied [3]. Using this approach, lower and upper bounds for the energy barriers of systems up to size $L = 40$ could be obtained. For the two bounds, respectively, a power law $E_{\mathrm{barrier}} \sim L^{\psi}$ was found with $\psi_{\mathrm{lower}} = 0.25$ and $\psi_{\mathrm{upper}} = 0.54$. Note that an exact treatment of such systems sizes is impossible with current algorithms since the barrier problem is NP-complete [66].

Matching algorithms were also used in several studies [2,12,81] to obtain evidence whether domain walls in two-dimensional SGs are SLE processes. These are, see the introduction by Cardy [25], domain-wall generating stochastic processes which are obtained via conformal mappings from random walks. Using this connection to conformal-field theory a relation between fractal dimension d^s of domain walls and stiffness exponent θ could be proposed [2]:

$$d^s - 1 = 3/[4(3+\theta)]\,, \tag{7}$$

which is compatible with the so-far obtained results for Gaussian disorder, also with the corresponding random-bond model [63]. Note that for the bimodal $\pm J$ model with $\theta_{bm} = 0$ one obtains $d^s = 1.25$ which is compatible with the lower and upper bounds [62]. Nevertheless, it was argued by

Fisch [33], that the derivation of Eq. (7) are based of non-vanishing spin-correlations, which is not the case for the bimodal model. An indeed, a direct test by Risau-Gusman and Romá [81], based on the (somehow less certain) value for the fractal dimension ($d^{\mathrm{s}}_{\mathrm{bm}} \approx 1.33$), indicated that the domain walls of the bimodal model may not be SLE processes.

Finally, some interesting GS quantities have been obtained exactly, which are not directly accessible to the matching approach. For example, the GS and domain-wall entropy of the bimodal model could be calculated by Fisch [32,33] using an exact Pfaffian approach, which was introduced by Galluccio et al. [38]. The same quantities were also exactly addressed by Aromsawa and Poulter [5] through applying a mapping to a fermion problem for reasonable system sizes $L \leq 256$. Within the same approach, the algebraic $R^{-\eta}$ decrease of the spin-correlation function could be obtained by Poulter and Blackman [78], leading to $\eta = 0.12$. Note that within the matching approach, only an estimate $\eta = 0.22$ could be given from studying droplet excitations [44].

4 Regular ferromagnet mixed with spin glass

The two-dimensional *randomly-coupled ferromagnet* (RCF) consists of ferromagnetic second-neighbor bonds of strength J and random nearest-neighbor bonds ($\pm\lambda J$) [47]. Previous results from ground-state calculations indicate that this system might exhibit an ordered spin-glass phase at low but nonzero temperature, i.e., $T_c > 0$. Nevertheless, the RCF is not a planar system, hence it cannot be studied using fast exact algorithms. The previous results were obtained for systems of limited size using a heuristic algorithm [40,41].

Here, a similar system is studied, which has the advantage that it is planar. Hence, the exact GS matching algorithms can be applied. Nevertheless it contains also two percolating sublattices, one ferromagnetic, and one with random bonds. The lattice consist of a quadratic sublattice with random bonds of magnitude λJ, with a fraction p of antiferromagnetic bonds and a fraction $(1-p)$ of ferromagnetic bonds. Furthermore, for each square plaquette, exactly on nearest neighbor ferromagnetic bond (strength J), connecting opposite corners of the plaquette, is present. The ferromagnetic bonds are arranged in an "alternating" way, such that a ferromagnetic square sublattice (with lattice constant $\sqrt{2}$ compared to the spin-glass sublattice) is created. In fact, the resulting lattice is a triangular lattice, with a special arrangement, see Fig. 9.

In the top of Fig. 10, the disorder average value of the stiffness energy is displayed for different values the relative strength λ of the SG bonds, for the case of antiferromagnetic and ferromagnetic bonds having the same probability $p = 1 - p = 0.5$. The average was performed for each considered combination of (L, λ) for at least 1000 independent realizations of the disorder. Obviously, for $\lambda < 1$, the stiffness increases, the ferromagnetic order dominates. For $\lambda \geq 1$, the stiffness decreases for large system sizes, no ferromagnetic order will be present at any nonzero temperature. Hence, this parameter range could be a candidate for a SG phase. Nevertheless, as the lower part of Fig. 10 shows, also the variance of the stiffness energies decreases for large enough system sizes in this case. In particular for $\lambda = 1$ this

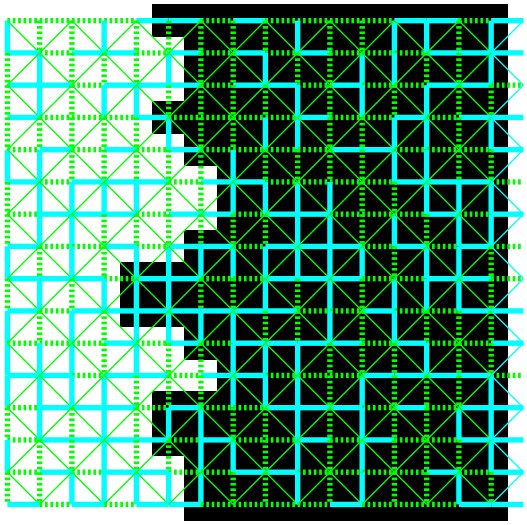

Fig. 9 A sample realization ($L = 16$). Thin diagonal (second-neighbor) bonds are ferromagnetic, the horizontal and vertical thick lines are either ferromagnetic (solid) or antiferromagnetic (dotted). The black and white squares in the background denote the result of a GS domain-wall calculation: black squares indicate spins which did not change by inverting the boundary conditions, while white squares indicate those spins which flipped.

finite-size effect appears particular strong. As a result, in the thermodynamic limit, no SG order seems to be present whenever no ferromagnetic order is present. This is on contrast to the result [47] for the RCF. Therefore, the model presented here, does not allow for an numerically efficient study of a system exhibiting SG order at some nonzero temperature. Recently, for another planar random Isign model, which was proposed to exhibit a stable SG phase, it could be shown [42] that $T_c = 0$ holds as well.

Nevertheless, the model is studied here in further detail for $\lambda = 1.0$, up to quite large systems sizes. For $L \leq 1024$ at least 4000 realizations were considered for each system size, 500 realizations for $L = 1448$. In Fig. 11 the variance of the stiffness energy is shown. Interestingly, for intermediate and large sizes, a power law behavior can be observed. From fitting the data in a range $L \in [40, 724]$ to a power law aL^{-b}, values $a = 29.3(9)$ and $b = 0.294(6)$ were obtained. In the present range, no crossover to a constant stiffness can be observed. If one expects that this takes place when $\mathrm{Var}(\Delta E) \approx 1$ is reached, like for the standard bimodal spin glass, then one has to reach system sizes of about $L = 10^6$, far out of reach of any known algorithm. Also the more efficient direct calculation of the partition function [90] does not allow to study such large system sizes. Hence, for this type of system, the finite-size effects are really huge.

We have seen that for the particular choice of $p = 0.5$ near $\lambda = 1.0$ no ferromagnetic as well as spin-glass order can be present at any nonzero temperature. This "critical" value of λ will probably depend on the value

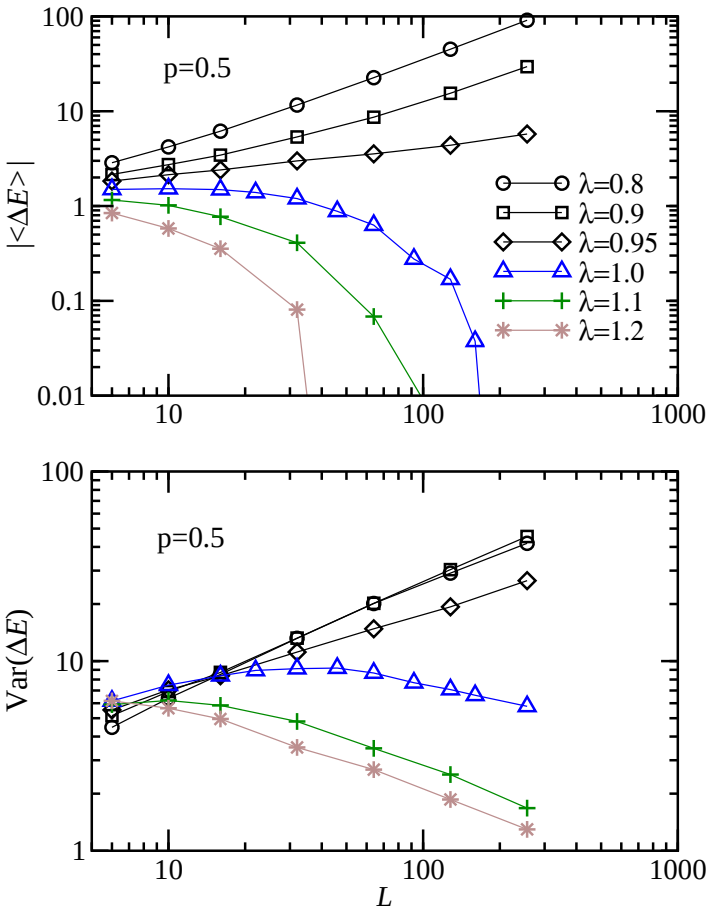

Fig. 10 Disorder average and empirical variance of the stiffness energy for $p = 0.5$ and different values of the relative strength λ of the SG bonds as a function of system size $L \in [6, 128]$. The lines are guides to the eyes only.

of p. Therefore, further simulations for different value of p were performed. In Fig. 12 $\lambda_c(p)$ is exposed. Note the $\lambda_c(p)$ is symmetric: If one performs a gauge transformation which multiplies every second spin in a checker-board manner by -1, then all diagonal ferromagnetic bonds remain ferromagnetic, but all random bonds switch sign. Hence, the situations at p and $1 - p$ are really equivalent, as for the original random-bond model: It exhibits for $p < p_c \approx 0.103$ only a ferromagnetic phase (and an antiferromagnetic phase for $p > 1 - p_c$) [55,1]. Hence, in about this region, where the concentration of frustrated plaquettes is small, also for the present model only the (anti-) ferromagnetic ordered phases should exist. Correspondingly, the value of λ_c strongly increasing, when approaching p_c and $1 - p_c$ from the intermediate region, respectively. Note that for $p > 1 - p_c$ a ferromagnet-antiferromagnet

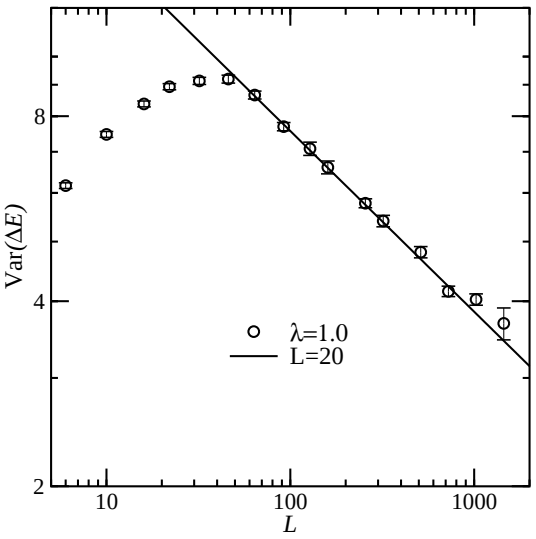

Fig. 11 Variance of the stiffness energy for $\lambda = 1.0, p = 0.5$ as a function of system size. The line shows a power law aL^{-b} with $a = 29.3$, $b = 0.286$.

transition should occur at some value of λ, which is not visible when calculating the stiffness energy.

5 Summary

The matching approach to the numerical calculation of spin-glass ground states for two-dimensional Ising spin glasses has been presented. This approach allows to calculate GSs of large samples exactly. A pedagogical introduction to these algorithms has been given here. Recently Pardella and Liers introduced modifications of the algorithms [76] which are able to handle systems of $N = 3000^2$ spins. The running time of the new approach seems to be comparable to the approach presented here, but maybe it consumes less memory. Nevertheless, the new approach has for sure the advantage that no weight limit $w_{\max}$ is necessary. Whether it is useful to calculate, e.g., droplet excitations, where the running time is the limit, is not clear. Nevertheless, since no extensive application to a physical problem has been published so far, the full potential of the new approach is still to be determined. Furthermore, Thomas and Middleton have presented [91] an approach which is able to treat systems with periodic boundary conditions of reasonable sizes up to $L = 400$.

Independently of the algorithm to actually calculate the GSs, using sophisticated extensions based on modifications of the samples after a first GS calculation, also various excitations like domain walls and droplets can be calculated. It is even possible to obtain low-energy paths in configuration space.

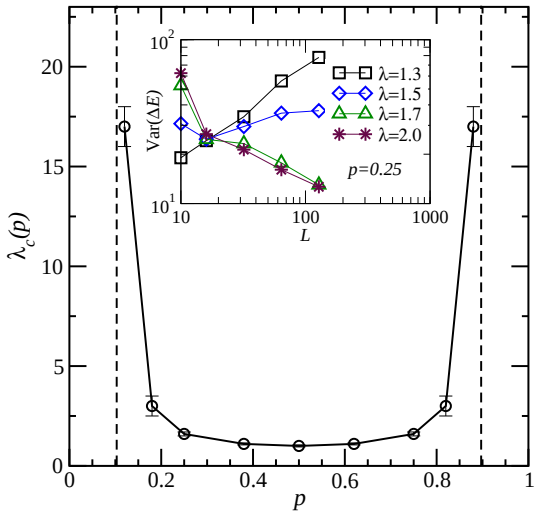

Fig. 12 Critical strength λ_c of the random interactions above which the order is destroyed as a function of the probability p for a antiferromagnetic bond. the dashed lines indicate the ferromagnet spin-glass transition points p_c and $1 - p_c$, respectively, of the standard random-bond model. Solid lines are guides to the eyes only. The inset shows the variance of the variance of stiffness energy for the case $p = 0.25$ for different values of λ, supporting the result $\lambda_c(0.25) = 1.6(1)$.

In recent years many predictions of the droplet theory could be verified for two-dimensional Ising spin glasses by applying these algorithms. In particular the low-energy behavior is basically determined by one single exponent θ. Therefore, one can say, the two-dimensional SG is understood well so far. Also the scaling of energy barriers and SLE properties of the model have been evaluated.

Finally, in the current work, also a mixture of a ferromagnet with a spin glass has been examined, which seemed to offer the possibility for a stable low-temperature spin-glass phase. Nevertheless, only for intermediate system sizes the results support this notion. One has to study fairly large system, which is necessary here due to very strong finite-site effects. This is indeed possible using the matching approach. By considering these results it appears likely that also for this model only at $T = 0$ spin-glass order exists.

6 Acknowledgements

The author thanky Oliver Melchert for critically reading the manuscript and for giving many useful comments. The simulations were performed at the GOLEM I cluster for scientific computing at the University of Oldenburg (Germany).

References

1. Amoruso, C., Hartmann, A.K.: Domain-wall energies and magnetization of the two-dimensional random-bond Ising model. Phys. Rev. B **70**, 134,425 (2004)
2. Amoruso, C., Hartmann, A.K., Hastings, M.B., Moore, M.A.: Conformal Invariance and SLE in Two-Dimensional Ising Spin Glasses. Phys. Rev. Lett. **97**, 267,202 (2006)
3. Amoruso, C., Hartmann, A.K., Moore, M.A.: Determining Energy Barriers by Iterated Optimization: The Two-Dimensional Ising Spin Glass. Phys. Rev. B **73**, 184,405 (2006)
4. Amoruso, C., Marinari, E., Martin, O.C., Pagnani, A.: Scalings of domain wall energies in two dimensional Ising spin glasses. Phys. Rev. Lett. **91**, 087,201 (2003)
5. Aromsawa, A., Poulter, J.: Domain wall entropy of the bimodal two-dimensional Ising spin glass. Phys. Rev. B **76**(6), 064,427 (2007). DOI 10.1103/PhysRevB.76.064427
6. Atisattapong, W., Poulter, J.: Excitations of the bimodal ising spin glass on the brickwork lattice. New Journal of Physics **11**(6), 063,039 (2009). URL http://stacks.iop.org/1367-2630/11/i=6/a=063039
7. Barahona, F.: On the computational complexity of Ising spin glass models. J. Phys. A **15**(10), 3241–3253 (1982)
8. Barahona, F., Maynard, R., Rammal, R., Uhry, J.: Morphology of ground states of a two dimensional frustration model. J. Phys. A **15**, 673 (1982)
9. Barthel, W., Hartmann, A.K.: Clustering analysis of the ground-state structure of the vertex-cover problem. Phys. Rev. E **70**, 066,120 (2004)
10. Bendisch, J.: Groundstate threshold pc in ising frustration systems on 2d regular lattices. Physica A **202**(1-2), 48 – 67 (1994)
11. Bendisch, J.: Groundstate threshold in triangular anisotropic ±J Ising models. Physica A **245**(3-4), 560 – 574 (1997)
12. Bernard, D., Le Doussal, P., Middleton, A.A.: Possible description of domain walls in two-dimensional spin glasses by stochastic loewner evolutions. Phys. Rev. B **76**(2), 020,403 (2007). DOI 10.1103/PhysRevB.76.020403
13. Berthier, L., Young, A.P.: Energetics of clusters in the two-dimensional Gaussian Ising spin glass. J. Phys. A: Math. Gen. **36**(43), 10,835 (2003). URL http://stacks.iop.org/0305-4470/36/i=43/a=011
14. Bieche, I., Maynard, R., Rammal, R., Uhry, J.P.: On the ground states of the frustration model of a spin glass by a matching method of graph theory. J. Phys. A **13**, 2553 (1980)
15. Binder, K., Young, A.: Spin-glasses: Experimental facts, theoretical concepts and open questions. Rev. Mod. Phys. **58**, 801 (1986)
16. Boettcher, S.: Low-temperature excitations of dilute lattice spin glasses. EPL (Europhys. Lett.) **67**(3), 453 (2004). URL http://stacks.iop.org/0295-5075/67/i=3/a=453
17. Boettcher, S., Hartmann, A.K.: Reduction of two-dimensional dilute Ising spin glasses. Phys. Rev. B **72**(1), 014,429 (2005). DOI 10.1103/PhysRevB.72.014429
18. Bouchaud, J.P., Krzakala, F., Martin, O.C.: Energy exponents and corrections to scaling in Ising spin glasses. Phys. Rev. B **68**, 224,404 (2003)
19. Bovier, A., Fröhlich, J.: A heuristic theory of the spin glass phase. J. Stat. Phys. **44**, 347–391 (1986)
20. Bray, A.J., Moore, M.A.: Lower critical dimension of Ising spin glasses: a numerical study. J. Phys. C **17** (1984)
21. Bray, A.J., Moore, M.A.: Chaotic nature of the spin-glass phase. Phys. Rev. Lett. **58**(1), 57–60 (1987). DOI 10.1103/PhysRevLett.58.57
22. Bray, A.J., Moore, M.A.: Scaling theory of the ordered phase of spin glasses. In: J.L. van Hemmen, I. Morgenstern (eds.) Heidelberg Colloquium on Glassy Dynamics, p. 121. Springer, Berlin (1987)
23. Campbell, I.A., Hartmann, A.K., Katzgraber, H.G.: Energy size effects of two-dimensional Ising spin glasses. Phys. Rev. B **70**, 054,429 (2004)
24. Cardy, J.: Scaling and Renormalization in Statistical Physics. Cambridge University Press, Cambridge (1996)

25. Cardy, J.: SLE for theoretical physicists. Annals of Physics **318**, 81–118 (2005)
26. Carter, A.C., Bray, A.J., Moore, M.A.: Aspect-ratio scaling and the stiffness exponent for Ising spin glasses. Phys. Rev. Lett. **88**, 077,201 (2002)
27. Cook, W., Rohe, A.: URL http://www2.isye.gatech.edu/ wcook/blossom4/. Calculation of minimum-weighted perfect matchings via the blossom4 extension to the Concorde library.
28. Cook, W.J., Cunningham, W.H., Pulleyblank, W.R., Schriever, A.: Combinatorial Optimization. Wiley, New York (1998)
29. Cormen, T.H., Clifford, S., Leiserson, C.E., Rivest, R.L.: Introduction to Algorithms. MIT Press, Cambridge (USA) (2001)
30. Derigs, U., Metz, A.: Solving (large scale) matching problems combinatorially. Math. Prog. **50**, 113 (1991)
31. Edwards, S.F., Anderson, P.W.: Theory of spin glasses. J. Phys. F **5**, 965 (1975)
32. Fisch, R.: Finite-size scaling of the domain wall entropy distributions for the 2d $\pm J$ Ising spin glass. J. Stat. Phys. **125**, 793 (2006)
33. Fisch, R.: Aspect-ratio scaling of domain wall entropy for the 2d $\pm J$ Ising spin glass. J. Stat. Phys. **130**, 561–569 (2008). URL http://dx.doi.org/10.1007/s10955-007-9436-4. 10.1007/s10955-007-9436-4
34. Fisch, R., Hartmann, A.K.: Ground-state and domain-wall energies in the spin-glass region of the 2d $\pm J$ random-bond Ising model. Phys. Rev. B **75**, 174,415 (2007)
35. Fischer, K.H., Hertz, J.A.: Spin Glasses. Cambridge University Press, Cambridge (1991)
36. Fisher, D.S., Huse, D.A.: Ordered phase of short-range Ising spin-glasses. Phys. Rev. Lett. **56**, 1601 (1986)
37. Fisher, D.S., Huse, D.A.: Equilibrium behavior of the spin-glass ordered phase. Phys. Rev. B **38**, 386 (1988)
38. Galluccio, A., Loebl, M., Vondrák, J.: New algorithm for the Ising problem: Partition function for finite lattice graphs. Phys. Rev. Lett. **84**(26), 5924–5927 (2000). DOI 10.1103/PhysRevLett.84.5924
39. Goldenfeld, N.: Lectures on phase transitions and the renormalization group. Addison-Wesely, Reading (MA) (1992)
40. Hartmann, A.K.: Cluster-exact approximation of spin glass ground states. Physica A **224**, 480–488 (1999)
41. Hartmann, A.K.: Scaling of stiffness energy for three-dimensional $\pm J$ Ising spin glasses. Phys. Rev. E **59**, 84 (1999)
42. Hartmann, A.K.: No spin-glass transition in the mobile-bond model. Phys. Rev. B **67**(21), 214,404 (2003). DOI 10.1103/PhysRevB.67.214404
43. Hartmann, A.K.: Domain walls, droplets and barriers in two-dimensional Ising spin glasses,. In: W. Janke (ed.) Rugged Free Energy Landscapes, Lecture Notes in Physics, pp. 67–106. Springer, Heidelberg (2007)
44. Hartmann, A.K.: Droplets in the two-dimensional $\pm J$ Ising spin glass. Phys. Rev. B **77**, 144,418 (2008)
45. Hartmann, A.K.: Practical Guide to Computer Simulations. World Scientific, Singapore (2009)
46. Hartmann, A.K., Bray, A.J., Carter, A.C., Moore, M.A., Young, A.P.: The stiffness exponent of two-dimensional Ising spin glasses for non-periodic boundary conditions using aspect-ratio scaling. Phys. Rev. B **66**, 224,401 (2002)
47. Hartmann, A.K., Campbell, I.A.: Ordered phase in the two-dimensional randomly coupled ferromagnet. Phys. Rev. B **63**, 094,423 (2001)
48. Hartmann, A.K., Moore, M.A.: Corrections to scaling are large for droplets in two-dimensional spin glasses. Phys. Rev. Lett. **90**, 12,720 (2003)
49. Hartmann, A.K., Moore, M.A.: Generating droplets in two-dimensional Ising spin glasses by using matching algorithms. Phys. Rev. B **69**, 104,409 (2004)
50. Hartmann, A.K., Rieger, H.: Optimization Algorithms in Physics. Wiley-VCH, Weinheim (2001)
51. Hartmann, A.K., Young, A.P.: Lower critical dimension of Ising spin glasses. Phys. Rev B **64**, 180,404 (2001)

52. Hartmann, A.K., Young, A.P.: Large-scale, low-energy excitations in the two-dimensional Ising spin glass. Phys. Rev B **65**, 094,419 (2002)
53. Kawashima, N.: Fractal droplets in two-dimensional spin glass. J. Phys. Soc. Jpn. **69**, 987 (2000)
54. Kawashima, N., Aoki, T.: Zero-temperature critical phenomena in two-dimensional spin glasses. J. Phys. Soc. Jpn. **69**, Suppl. A, 169 (2000)
55. Kawashima, N., Rieger, H.: Finite-size scaling analysis of exact gss for +or-j spin glass models in two dimensions. Europhys. Lett. **39**, 85 (1997)
56. Korte, B., Vygen, J.: Combinatorial Optimization – Theory and Algorithms. Springer, Springer (2000)
57. Landau, D.P., Binder, K.: Monte Carlo Simulations in Statistical Physics. Cambridge University Press, Cambridge (2000)
58. Landry, J.W., Coppersmith, S.N.: Ground states of two-dimensional $\pm J$ Edwards-Anderson spin glasses. Phys. Rev. B **65**, 134,404 (2002)
59. McMillan, W.L.: Domain-wall renormalization-group study of the two-dimensional random ising model. Phys. Rev. B **29**(7), 4026–4029 (1984). DOI 10.1103/PhysRevB.29.4026
60. McMillan, W.L.: Scaling theory of Ising spin glasses. J. Phys. C **17**, 3179 (1984)
61. Mehlhorn, K., Näher, S.: The LEDA Platform of Combinatorial and Geometric Computing. Cambridge University Press, Cambridge (1999). URL http://www.algorithmic-solutions.de
62. Melchert, O., Hartmann, A.K.: Fractal dimension of domain walls in two-dimensional Ising spin glasses. Phys. Rev. B **76**, 174,411 (2007)
63. Melchert, O., Hartmann, A.K.: Scaling behavior of domain walls at the $T = 0$ ferromagnet to spin-glass transition. Phys. Rev. B **79**, 184,402 (2009)
64. Melchert, O., Hartmann, A.K.: A dedicated algorithm for calculating ground states for the triangular random bond Ising model. Comp. Phys. Commun. p. in press (2011)
65. Mézard, M., Parisi, G., Virasoro, M.: Spin glass theory and beyond. World Scientific, Singapore (1987)
66. Middleton, A.A.: Computational complexity of determining the barriers to interface motion in random systems. Phys. Rev. E **59**(3), 2571–2577 (1999). DOI 10.1103/PhysRevE.59.2571
67. Middleton, A.A.: Numerical investigation of the thermodynamic limit for ground states in models with quenched disorder. Phys. Rev. Lett. **83**(8), 1672–1675 (1999). DOI 10.1103/PhysRevLett.83.1672
68. Middleton, A.A.: Energetics and geometry of excitations in random systems. Phys. Rev. B **63**(6), 060,202 (2001). DOI 10.1103/PhysRevB.63.060202
69. Newman, C.M., Stein, D.L.: Finite-dimensional spin glasses: states, excitations and interfaces. Annales Henri Poincaré **4**, S497–S503 (2003)
70. Newman, M.E.J., Barkema, G.T.: Monte Carlo Methods in Statistical Physics. Clarendon Press, Oxford (1999)
71. Ohzeki, M., Nishimori, H.: Analytical evidence for the absence of spin glass transition on self-dual lattices. Journal of Physics A: Mathematical and Theoretical **42**(33), 332,001 (2009). URL http://stacks.iop.org/1751-8121/42/i=33/a=332001
72. Ozeki, Y.: Ground state properties of the $\pm J$ Ising model in two dimensions. J. Phys. Soc. Jpn. **59**, 3531 (1990)
73. Palassini, M., Young, A.P.: Evidence for a trivial ground-state structure in the two-dimensional Ising spin glass. Phys. Rev. B **60**(14), R9919–R9922 (1999). DOI 10.1103/PhysRevB.60.R9919
74. Palassini, M., Young, A.P.: Nature of the spin glass state. Phys. Rev. Lett. **85**, 3017 (2000)
75. Palmer, R.G., Adler, J.: Ground states of large samples of two-dimensional Ising spin glasses. Int. J. Mod. Phys. C **10**, 667 (1999)
76. Pardella, G., Liers, F.: Exact ground states of large two-dimensional planar Ising spin glasses. Phys. Rev. E **78**, 056,705 (2008)
77. Picco, M., Ritort, F., Sales, M.: Statistics of lowest droplets in two-dimensional Gaussian Ising spin glasses. Phys. Rev. B **67**(18), 184,421 (2003). DOI 10.1103/PhysRevB.67.184421

78. Poulter, J., Blackman, J.A.: Exact algorithm for spin-correlation functions of the two-dimensional $\pm J$ Ising spin glass in the ground state. Phys. Rev. B **72**, 104,422 (2005)
79. Ramirez-Pastor, A.J., Rom, F., Nieto, F., Vogel, E.E.: Effect of the ground-state structure on order parameters in $\pm J$ ising lattices. Physica A: Statistical and Theoretical Physics **336**(3-4), 454 – 460 (2004). DOI DOI: 10.1016/j.physa.2003.12.038
80. Rieger, H., Santen, L., Blasum, U., Diehl, M., Jünger, M., Rinaldi, G.: The critical exponents of the two-dimensional Ising spin glass revisited: exact ground-state calculations and Monte Carlo simulations. J. Phys. A **29**, 3939 (1996)
81. Risau-Gusman, S., Romá, F.: Fractal dimension of domain walls in the Edwards-Anderson spin glass model. Phys. Rev. B **77**(13), 134,435 (2008). DOI 10.1103/PhysRevB.77.134435
82. Romá, F., Risau-Gusman, S., Ramirez-Pastor, A.J., Nieto, F., Vogel, E.E.: Influence of the ground-state topology on domain-wall energy in the Edwards-Anderson $\pm j$ spin glass model. Phys. Rev. B **75**(2), 020,402 (2007). DOI 10.1103/PhysRevB.75.020402
83. Romá, F., Risau-Gusman, S., Ramirez-Pastor, A.J., Nieto, F., Vogel, E.E.: The ground state energy of the edwards-anderson spin glass model with a parallel tempering Monte Carlo algorithm. Physica A: Statistical Mechanics and its Applications **388**(14), 2821 – 2838 (2009). DOI DOI: 10.1016/j.physa.2009.03.036
84. Romá, F., Risau-Gusman, S., Ramirez-Pastor, A.J., Nieto, F., Vogel, E.E.: Ground-state topology of the edwards-anderson $\pm j$ spin glass model. Phys. Rev. B **82**(21), 214,401 (2010). DOI 10.1103/PhysRevB.82.214401
85. Sedgewick, R.: Algorithms in C. Addison-Wesley, Reading (MA) (1990)
86. Sherrington, D., Kirkpatrick, S.: Solvable model of a spin glass. Phys. Rev. Lett. **35**, 1792 (1975)
87. Simone, C., Diehl, M., Jünger, M., Mutzel, P., Reinelt, G., Rinaldi, G.: Exact ground states of Ising spin glasses: New experimental results with a branch-and-cut algorithm. J. Stat. Phys. **80**, 487–496 (1995). URL http://dx.doi.org/10.1007/BF02178370. 10.1007/BF02178370
88. Simone, C., Diehl, M., Jünger, M., Mutzel, P., Reinelt, G., Rinaldi, G.: Exact ground states of two-dimensional $\pm J$ Ising spin glasses. J. Stat. Phys. **84**, 1363–1371 (1996). URL http://dx.doi.org/10.1007/BF02174135. 10.1007/BF02174135
89. Swamy, M.N.S., Thulasiraman, K.: Graphs, Networks and Algorithms. Wiley, New York (1991)
90. Thomas, C.K., Huse, D.A., Middleton, A.A.: Zero and low temperature behavior of the two-dimensional $\pm J$ Ising spin glass. preprint arXiv:1103.1946 (2011)
91. Thomas, C.K., Middleton, A.A.: Matching kasteleyn cities for spin glass ground states. Phys. Rev. B **76**, 220,406R (2007)
92. Weigel, M., Johnston, D.: Frustration effects in antiferromagnets on planar random graphs. Phys. Rev. B **76**(5), 054,408 (2007). DOI 10.1103/PhysRevB.76.054408